

# Electrochemical study of a SOFC fuelled with various gaseous mixtures issued from biomass gasification

A. Le Gal La Salle<sup>1</sup>, F. Ricoul<sup>1</sup>, O. Joubert<sup>1</sup>, A. Kerihuel<sup>2</sup>, A. Subrenat<sup>3</sup>

<sup>1</sup>IMN, 2 rue de la Houssinière 44322 Nantes, France

<sup>2</sup>S3D, 2 rue Alfred Kastler 44307 Nantes, France

<sup>3</sup>EMN, 4 rue Alfred Kastler 44307 Nantes, France

Annie.legal@cnrs-immn.fr

**Keywords: Solid Oxide Fuel Cells, Fueling conditions, Electrochemical Impedance Spectroscopy (EIS)**

The main advantage of SOFCs is the flexibility of the fuel: hydrogen, natural gas, but also renewable gas extracted from biomass. The VALORPAC project, supported by ADEME and gathering the four partners IMN, S3D, Fiaxell and Syngaz, consists in fueling a SOFC with a gas produced by a wood gasifier. This is not only hydrogen and carbon monoxide (syngaz) but a complex mixture constituted mainly by nitrogen, carbon dioxide, water vapor, methane, hydrogen chloride sulfide. Detailed studies of the power and EIS response of SOFC fueled by different synthetic mixtures with compositions close to those of the product of the gasifier are presented in this communication. The concept is validated at 710°C, using wet (3% H<sub>2</sub>O) derived syngas (17% H<sub>2</sub> / 20% CO / 3% CH<sub>4</sub> / 60% N<sub>2</sub> and 17% H<sub>2</sub> / 20% CO / 3% CH<sub>4</sub> / 10% CO<sub>2</sub> / 50% N<sub>2</sub>) on the anode side of SOFC cells (Figure 1). As shown on Figure 1, the U/J responses of the cells obtained with various fueling conditions are completed with electrochemical impedance diagrams, allowing the investigation of the differences in mechanisms occurring at the electrodes which will be presented in this communication.

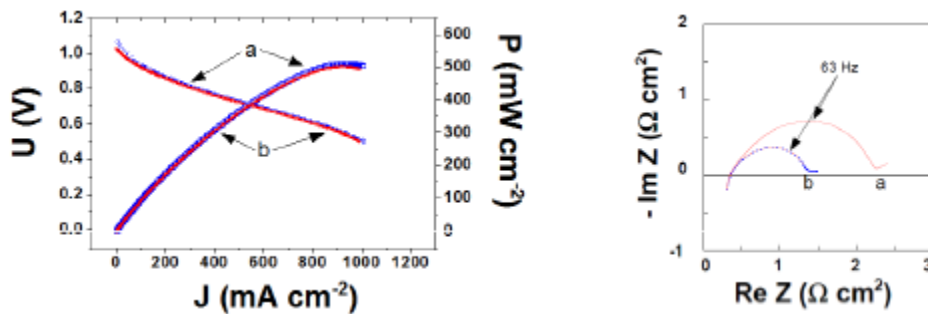


Figure 1. Voltage and power density versus current density characteristics recorded at 10 mV s<sup>-1</sup> (left) and Nyquist diagrams (right) at OCV of the cell 107.10 at 750°C under air on the cathode side and wet (3% H<sub>2</sub>O) 17% H<sub>2</sub> - 20% CO - 3% CH<sub>4</sub> - 60% N<sub>2</sub> mixture (a) and 17% H<sub>2</sub> - 20% CO - 3% CH<sub>4</sub> - 10% CO<sub>2</sub> - 50% N<sub>2</sub> (b) on the anode side. Numbers mentioned above the Nyquist diagram are the frequency values.

## REFERENCE

1. F. Ricoul, A. Le Gal La Salle, A. Subrenat, O. Joubert et A. Kerihuel, *International Discussion on Hydrogen Energy and Applications*, Nantes, 12-14 mai 2014.

# Electrochemical study of a SOFC fuelled with various gaseous mixtures issued from biomass gasification

A. Le Gal La Salle<sup>1</sup>, F. Ricoul<sup>1</sup>, O. Joubert<sup>1</sup>, A. Kerihuel<sup>2</sup>, A. Subrenat<sup>3</sup>

<sup>1</sup>IMN, 2 rue de la Houssinière 44322 Nantes, France

<sup>2</sup>S3D, 2 rue Alfred Kastler 44307 Nantes, France

<sup>3</sup>EMN, 4 rue Alfred Kastler 44307 Nantes, France

*annie.legal@cnrs-immn.fr*

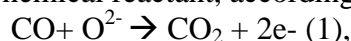
**Keywords: Solid Oxide Fuel Cells, Fueling conditions, Electrochemical Impedance Spectroscopy (EIS)**

## ABSTRACT

This work focuses on the role of CO and CO<sub>2</sub> commonly present in syngas generated by biomass gasification when they are flowed in a Ni-YSZ-based SOFC. Polarization, power versus intensity and electrochemical impedance spectroscopy measurements are performed both at Open Circuit Voltage (OCV) and under polarization. The H<sub>2</sub>-CO-CO<sub>2</sub> mixture is a convenient electrochemical reactant, even in the presence of a small amount of CH<sub>4</sub>. A power density value of 502 mW cm<sup>-2</sup> is obtained at 750°C when the cell is fueled with a 50% N<sub>2</sub>-20% CO-17% H<sub>2</sub>-10% CO<sub>2</sub>-3% CH<sub>4</sub> mixture, which appears to be a realistic composition corresponding to the exhaust of the gasifier. Studies reveal also that under polarization, the resistance of the cell is mainly due to electrolyte.

## 1. INTRODUCTION

Energy transition involves using a mix of renewable energy including biomass. Reusable gases can be extracted from that biomass [1]. Currently, more heat power than electrical power is produced from that source. Nevertheless, in order to improve the electric yield and to avoid noxious gases, the gas conversion into electricity can be operated by solid oxide fuel cell (SOFC) [2-5]. These kinds of fuel cell can double the electric yield and cogeneration is possible thanks to high operating temperatures (700°C-900°C), which increases the global yield. This work is a part of the VALORPAC project, which consists in integrating a SOFC in a gasification process. In this project, the power source is produced by a fixed bed downdraft wood gasifier. Indeed, this type of gasifier is known to produce cleaner syngas with low tars rate compared to updraft or fluidized bed reactors [6], and S3D has patented recently (n° PCT/FR2011/052318) a gasifier reactor specially designed to produce high quality syngas which could be used nearly directly to fuel a SOFC. Indeed experimental tests were done with wood pellets and wood chips, and preliminary measurements of the composition of the corresponding gasifier exhaust are given in Table 1 [7,8]. Usually SOFC are fueled with hydrogen and their operation is known to be dependent on any pollutant [5,7]. Indeed the aim of the study is to explore the electrochemical response of the cells used in the project when they are fueled by the gas issued from the wood gasifier patented by S3D, i.e. a mixture of N<sub>2</sub>, H<sub>2</sub>, CO and CO<sub>2</sub>, in presence of small amounts of CH<sub>4</sub>. In a previous paper [9], the potential use of Fiaxell YSZ-based solid oxide fuel cells with different H<sub>2</sub>-CO-CO<sub>2</sub>-N<sub>2</sub> mixtures, containing small amounts of CH<sub>4</sub>, has been checked in the 750°C-850°C range. It has been shown that in these conditions the presence of carbon oxides CO<sub>2</sub> and CO do not damage the cell. Indeed, CO is a real electrochemical reactant, according to reaction (1):



leading in some cases to higher power densities than H<sub>2</sub>, for instance at 750°C when it is mixed with N<sub>2</sub> at percentage lower than 27%. Impedance measurements at OCV showed that this limitation of acceptable amount of CO is due to mass transfer limitations, evidenced at OCV. Results showed also that CO<sub>2</sub>, which is produced by the CO oxidation but which is also present in the gaseous mixtures issued from the gasifier, acts both in reducing the OCV voltage, and then the slope of the U/J curve and corresponding total cell resistance, but also as a reactant in the water gas shift equilibrium (2), with a possible decrease of the cell properties if the transformation of H<sub>2</sub> into CO is too important.



In this paper, these preliminary results are extended to a more large temperature range, and completed by electrochemical measurements realized under polarization, i.e. in conditions corresponding to realistic cell operation conditions.

Table 1. Average amounts of the main components measured in the gas issued from the gasifier [8]

Component	Amount
N <sub>2</sub>	45-55 % vol.
H <sub>2</sub>	15-20 % vol.
CO	15-25 % vol.
CO <sub>2</sub>	10-15 % vol.
CH <sub>4</sub>	<3 % vol.
H <sub>2</sub> O	5-15 % vol.
Tars and particles	<1g/Nm <sup>3</sup>

## 2. EXPERIMENTAL

### 2.1. Cell

The SOFC is a Fiaxell circular shaped planar anode-supported 2R-Cell™ [10] composed of commonly used materials, i.e. a Ni/Yttria-Stabilized Zirconia (YSZ) anode, prepared in situ by reduction of a YSZ/NiO cermet, an YSZ electrolyte covered by a Gadolinium-Doped Ceria layer GDC containing cobalt oxide, and a La<sub>0.6</sub>Sr<sub>0.4</sub>CoO<sub>3-δ</sub> 10 cm<sup>2</sup> area cathode.

### 2.2. Apparatus and temperature program

The experimental setup, provided by Fiaxell, is described in [10]. At the anode side the selected mixture of gas among CO or CO<sub>2</sub>, H<sub>2</sub>, N<sub>2</sub> and CH<sub>4</sub> is flowed. Each gas is controlled by flowmeters and bubbles in water at room temperature (pH<sub>2</sub>O=0.3 atm) for the whole mixture. The total anode flow is always set to 200 ml min<sup>-1</sup>. The fuel cells are submitted to the following temperature program: ramp 120°C h<sup>-1</sup> until the temperature reaches 620°C at the thermocouple, under 250 ml.min<sup>-1</sup> air (fixed value for the entire study) and 200 ml min<sup>-1</sup> N<sub>2</sub>. Then at the 620°C stage, 10 ml min<sup>-1</sup> H<sub>2</sub> and 190 ml min<sup>-1</sup> N<sub>2</sub> are provided during 15 hours, in order both to achieve the sintering of the cathode and to activate the anode by reducing NiO to Ni. The final measurement temperature is reached after a 120°C h<sup>-1</sup> ramp at the same gas flow, and the cell is fueled with the chosen gas mixture.

### 2.3. Polarization curves and Electrochemical Impedance Spectroscopy

Current collectors, made of discs of gold grid connected to the cathode and of nickel grid connected with the anode, are used. Polarization curves are obtained by the Versastat device and the associated software VersaStudio from Princeton Applied Research in linear square wave voltammetry mode at the 1 mv s<sup>-1</sup> scan rate. Electrochemical impedance spectroscopy

was performed at the OCV or 0.8V by a device called VersaStat and the associated software VersaStudio from Princeton Applied Research, in potentiostatic EIS mode, start frequency 10000 Hz, end frequency 0.1 Hz and 20 mV or 10 mV as amplitude of the perturbation signal. This value has been optimized to meet the linearity requirement of the transfer function [11]. The impedance data were analyzed using ZView2-Software [12].

### 3. RESULTS AND DISCUSSION

#### 3.1. Results obtained by fueling the cell with $H_2 - N_2$ mixtures.

##### 3.1.1. Influence of the temperature.

Figure 1 shows the voltage (A) and power density (B) versus current density characteristics obtained at different temperatures under wet (3%  $H_2O$ ) 40%  $H_2$ -60%  $N_2$  mixture on the anode side at  $10 \text{ mV s}^{-1}$ . As already published in [9], the Open Circuit Voltage (OCV) is higher when the temperature is smaller, but the slope of the curve at the origin is also higher, leading finally to a crossing of the curves, already observed in literature [13], and to an increase of the intensity of the peak power density with temperature. Values collected in Table 2 compete favorably with published values obtained in similar conditions [14]. It can be noted that the use of redox-tolerant Fiaxell cells allows to decrease the voltage drastically, and to obtain important Fuel Utilization (FU) percentages (Table 2), reaching 89% for  $800^\circ\text{C}$ . In these conditions, the amount of water produced is considerable, and the quantity introduced with the fuel becomes negligible towards the amount produced in situ.

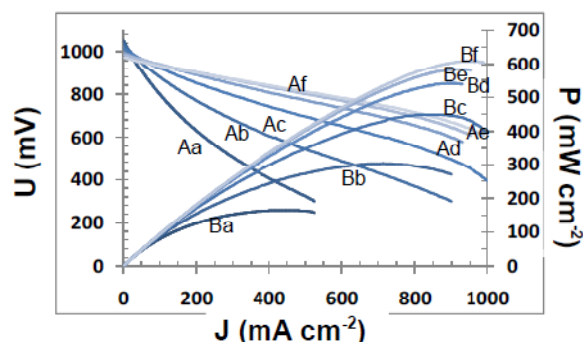


Figure 1: Voltage (A) and power density (B) versus current density characteristics at  $600^\circ\text{C}$  (a),  $650^\circ\text{C}$  (b),  $700^\circ\text{C}$  (c),  $750^\circ\text{C}$  (d),  $800^\circ\text{C}$  (e) and  $855^\circ\text{C}$  (f) under wet (3%  $H_2O$ ) 40%  $H_2$ -60%  $N_2$  mixture on the anode side and air on the cathode side and at  $10 \text{ mV s}^{-1}$ .

Table 1. Maximum power densities (PD) and corresponding Fuel Utilization (FU) values recorded for different fueling conditions (expressed in percentages) at different temperature T.

	$40H_2/60N_2$		$20H_2/80N_2$		$20H_2/20CO/10CO_2/50N_2$	
T ( $^\circ\text{C}$ )	PD ( $\text{mW cm}^{-2}$ )	FU (%)	PD ( $\text{mW cm}^{-2}$ )	FU (%)	PD ( $\text{mW cm}^{-2}$ )	FU (%)
600	165	43	137	53	136	37
650	303	68	209	72	267	62
700	449	81	261	81	397	77
750	541	85	300	86	482	82
800	584	89	323	95	537	85
850	609	89	317	95	568	86

Impedance diagrams were plotted at each temperature at OCV and at 800 mV. At OCV, and for temperatures comprised between 750°C and 850°C, as illustrated with curve (a) of Figure 2, the diagram is mainly composed of two depressed semi-circles and can be fitted by the electrical equivalent circuit  $L + R1 + (R2//CPE2) + (R3//CPE3)$  [15] represented on Fig 2B. At lower temperatures, as shown on curve (b) of Figure 2, the first loop is more depressed, and the diagram must be fitted by the electrical equivalent circuit  $L + R1 + (R2A//CPE2A) + (R2B//CPE2B) + (R3//CPE3)$ . The inductance  $L$ , related to the wires, ranges between 0.9 and  $1.1 \cdot 10^{-6}$  H, in accordance with literature with a similar testing set-up [16]. As already published in [9], the series resistance  $R1$ , which increases from 0.19 to 1.28 when the temperature decreases from 850 to 600°C, is mainly due to the electrolyte resistance, and is in accordance with reported values for GDC/YSZ electrolytes [17]. The impedance formula of the Constant Phase Element (CPE), which often characterizes inhomogeneous electrodes, is  $1/Q(j\omega)^n$ , with an associated capacitance  $C$  calculated from the formula  $(RC)^n=RQ$  [18]. The calculated capacitance values of the  $R2A//CPE2A$ ,  $R2B//CPE2B$  and  $R3//CPE3$  or  $R2//CPE2$  and  $R3//CPE3$  circuits are respectively comprised in the  $1 \cdot 10^{-3}$ - $5 \cdot 10^{-3}$ ,  $1 \cdot 10^{-2}$ - $5 \cdot 10^{-2}$  and  $0.7$ - $0.9 \text{ F cm}^{-2}$  ranges or  $9 \cdot 10^{-3}$ - $2 \cdot 10^{-2}$  and  $0.7$ - $0.9 \text{ F cm}^{-2}$  ranges. Comparing those values to values reported in previously published studies of similar electrode materials used in comparable conditions, it is possible to attribute the three circuits to mass transfer phenomena [19-21].

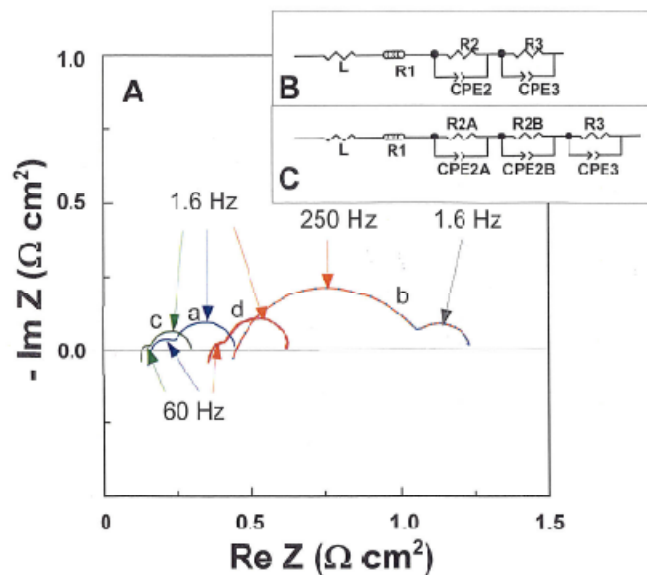


Figure 2: Nyquist diagrams (A) recorded at OCV at 850°C (a) and 700°C (b), and at 0.8V at 850°C (c) and 700°C (d) under wet (3% H<sub>2</sub>O) 40% H<sub>2</sub>-60% N<sub>2</sub> mixture on the anode side. Numbers mentioned above the diagram are the frequency values. (B) and (C) are equivalent circuit used for fitting the impedance diagrams (details are given in text).

Curve (a) of Figure 3A presents the variations with temperature of  $R2$  or  $(R2A+R2B)$  values measured at OCV. It demonstrates that the associated phenomena are thermodynamically activated. On the contrary  $R3$  is unchanged with temperature (curve (b) of Figure 3A), suggesting that it is associated to a phenomenon which is not dependent on temperature, such as diffusion [14,22].

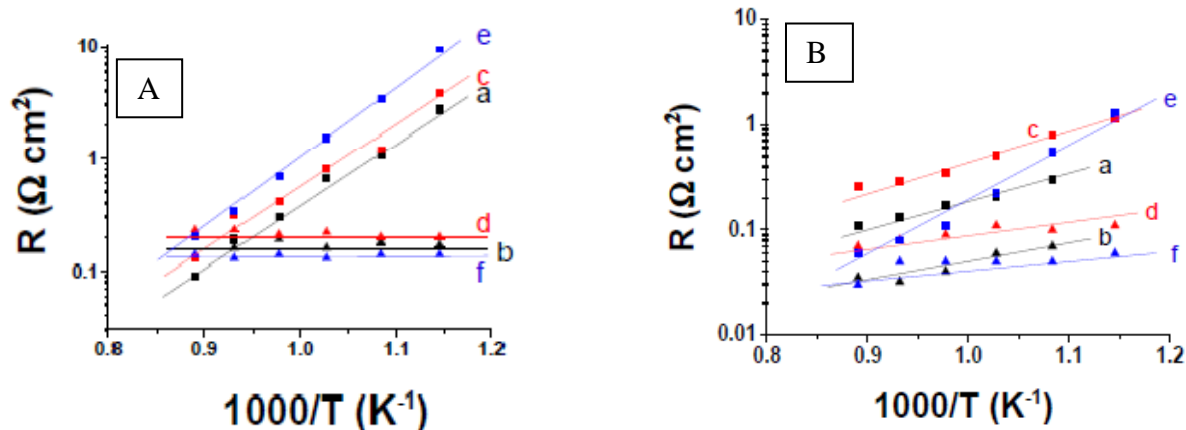


Figure 3: Variations with temperature of resistance values measured at OCV (A) and at 0.8V (B) for cell fueled with wet (3%  $\text{H}_2\text{O}$ ) 40%  $\text{H}_2$ -60%  $\text{N}_2$  mixture (R2 or R2A+R2B (a) et R3 (b)), wet (3%  $\text{H}_2\text{O}$ ) 20%  $\text{H}_2$ -80%  $\text{N}_2$  mixture (R2 or R2A+R2B (c) and R3 (d)) and wet (3%  $\text{H}_2\text{O}$ ) 20%  $\text{H}_2$ -20%  $\text{CO}$ -10%  $\text{CO}_2$ -50%  $\text{N}_2$  mixture (R2 or R2A+R2B (e) and R3 (f)).

The intersection of the low frequency part of the diagram with the real axis allows the determination of the total resistance of the cell and impedance measurements allow also to determine  $R_1/R_p$  and  $(R_p - R_1)/R_p$  values, corresponding respectively to the contribution of the electrolyte and of the electrodes to the total resistance  $R_p$  of the cell. When increasing temperature, the increase of the YSZ conductivity is less important than the thermal activation of the reaction taking place at the electrodes, resulting in a slight decrease of the contribution of the electrodes from 70 to 60%.

At 0.8V, and for all temperatures, as illustrated with curves (c) and (d) of Figure 2, the diagram is mainly composed of two depressed semi-circles and can be fitted by the electrical equivalent circuit  $L + R_1 + (R_2//CPE_2) + (R_3//CPE_3)$  of Fig 2B. The calculated capacitance values of the  $R_2//CPE_2$  and  $R_3//CPE_3$  circuits are respectively comprised in the  $10^{-3} - 10^{-2}$  and 0.7-1.1  $\text{F cm}^{-2}$  ranges, and the corresponding  $R_2$  and  $R_3$  values are lower than at OCV. Moreover, the variations of  $R_2$  with  $T$ , presented in curve (a) of Figure 3B are less important than at OCV, and the  $R_3$  value (curve (b) of Figure 3B) seems depend slightly on the temperature. At 0.8V, the part of the resistance of the cell due to electrolyte is drastically more important than at OCV, and when increasing temperature the increase of the YSZ conductivity is more important than the thermal activation of the reactions taking place at the electrodes, resulting in this case of an increase of the contribution of the electrodes from 35 to 42%.

### 3.1.2. Influence of the the percentage of $\text{H}_2$ in $\text{H}_2 - \text{N}_2$ mixture.

Experiments were realized by fueling the cell with a wet (3%  $\text{H}_2\text{O}$ ) 20%  $\text{H}_2$ -80%  $\text{N}_2$  mixture. The voltage and power density versus current density curves are similar than those of Figure 1, but OCV, and also the voltage observed at each current density value, are lower, leading to lower power densities values, as quantified in table 2. The Fuel Utilization measured at the maximum of the power versus current density curves is slightly higher than for 40% of  $\text{H}_2$ , and increases from 53 to 95% when the temperature increases from 600 to 850°C.

Impedance diagrams were plotted at OCV at different temperatures. As shown on curves (c) and (d) of Figure 3A, the decrease of the amount of active fuel results in an increase of both

the R2 (or (R2A+R2B) at temperatures lower than 750°C) and R3 values, and confirms that these resistances are both gas dependant as it is the case for mass transfer phenomena [23]. As a consequence, the contribution of the electrodes to the total resistance Rp of the cell is more important, varying from 76 to 66% when the temperature increases from 600 to 850°C. As it was observed for the 40%H<sub>2</sub>-60%N<sub>2</sub> mixture, the R2 and R3 values (curve (c) and (d) of Figure 3B) are less important at 0.8 V than at OCV. Nevertheless, the decrease of the H<sub>2</sub> amount of the fueling gas results in a drastic increase of both R2 and R3, and in this case, the contribution of the electrodes to the total resistance Rp of the cell is more important, varying from 50 to 63% when the temperature increases from 600 to 850°C.

### 3.2. Results obtained with fueling cells with CO - H<sub>2</sub>- CO<sub>2</sub> - CH<sub>4</sub> - N<sub>2</sub> mixtures.

Results obtained by fueling the cell with a wet (3% H<sub>2</sub>O) 20%H<sub>2</sub>-20%CO-10%CO<sub>2</sub>-50%N<sub>2</sub> mixture are presented in Table 2. The maximum power density and corresponding Fuel Utilization values are lower than for the 40%H<sub>2</sub>-60%N<sub>2</sub>, in accordance with the previously published work [9] establishing that CO is a better reactant than H<sub>2</sub>, but only in small quantities. Indeed, it explains why, in spite of the best results obtained with 20%H<sub>2</sub>-20%CO-60%N<sub>2</sub> compared to 40%H<sub>2</sub>-60%N<sub>2</sub>, the addition of CO<sub>2</sub> to the 20%CO/20%H<sub>2</sub> mixture, which can produce additional quantity of CO, leads finally to a slight decrease of the cell performance.

Impedance diagrams were plotted at OCV at different temperatures, and are similar to those of Figure 2, with similar capacitance values. As shown on curves (e) and (f) of Figure 3A, the presence of CO results mainly in an important increase of R2 (or (R2A+R2B) at temperatures lower than 750°C), and the contribution of the electrodes to the total resistance Rp of the cell vary from 82 to 64% when the temperature increases from 600 to 850°C. Moreover, the R2 and R3 values are drastically less important at 0.8 V (curves (e) and (f) of Figure 3B) than at OCV, and in this case, the contribution of the electrodes to the total resistance Rp of the cell vary from 51 to 30% when the temperature increases from 600 to 850°C.

The gas issued from the S3D's gasifier contains a small amount of CH<sub>4</sub> (Table 1) which can influence SOFC operation [24]. Cell performance has been measured at 750°C [9] when wet (3% H<sub>2</sub>O) 17% H<sub>2</sub>-20% CO-3%-CH<sub>4</sub>-60% N<sub>2</sub> is used as fuel. The power density value reaches a maximum of 512 mW cm<sup>-2</sup>, and suggests a complete CH<sub>4</sub> reforming according to reaction (3), favored by the important water formation due to the simultaneous oxidation of the 17% H<sub>2</sub> - 20% CO present in the mixture.



With 10% CO<sub>2</sub> in the fuel (which is then composed of wet (3% H<sub>2</sub>O) 17% H<sub>2</sub> - 20%CO - 3% CH<sub>4</sub> - 10% CO<sub>2</sub> - 50% N<sub>2</sub>), a voltage decrease, more important near the OCV, and inducing a small decrease of the maximum power density values (502 mW cm<sup>-2</sup>), is observed. This result is also confirmed by the comparison of the two Nyquist diagrams of the Figure 5A obtained at OCV, which illustrates the decrease of the Rp values associated to the presence of CO<sub>2</sub>, due to the decrease of R2 and R3. For the wet (3% H<sub>2</sub>O) 17%H<sub>2</sub>-20%CO-3%CH<sub>4</sub>-60%N<sub>2</sub>, the contribution of the electrodes to the total resistance of the cell is of 89%, and decrease to 80% in the presence of CO<sub>2</sub>. The R2 and R3 values are drastically less important at 0.8 V (curves (a) and (b) of Figure 5B) than at OCV, and in this case the presence of CO<sub>2</sub> has no influence, with a contribution of the electrodes to the total resistance Rp of the cell of only 30%.

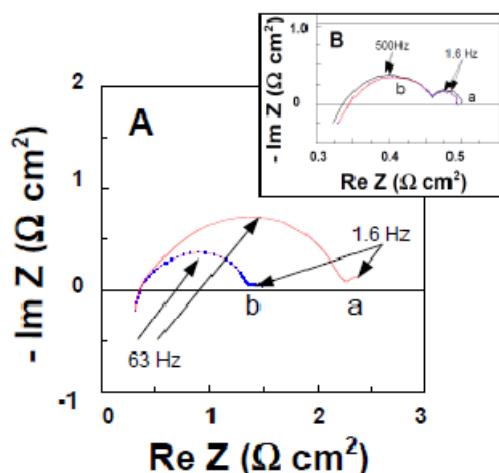


Figure 5: Nyquist diagrams recorded at 750 °C and at OCV (A) and at 0.8V (B), under wet (3% H<sub>2</sub>O) 17% H<sub>2</sub>-3% CH<sub>4</sub>-20%CO-60% N<sub>2</sub>, (a) and under wet (3% H<sub>2</sub>O) 17% H<sub>2</sub>-3% CH<sub>4</sub>-20%CO-10%CO<sub>2</sub>-50% N<sub>2</sub> (b). Numbers mentioned above the diagram are the frequency values.

## CONCLUSION

In this study, the potential use of Fiaxell YSZ-based solid oxide cell with wet H<sub>2</sub>-CO-CO<sub>2</sub>-CH<sub>4</sub>-N<sub>2</sub> mixtures, corresponding to the exhaust of the fixed bed downdraft S3D gasifier, has been confirmed in the whole 600°C-850°C range. Additional experiments are still in progress in order to study more precisely the ageing of the cells under these H<sub>2</sub>-CO-CO<sub>2</sub>-CH<sub>4</sub>-N<sub>2</sub> mixtures, and the effect of small amounts of H<sub>2</sub>S and HCl, which are also present in the exhaust of the gasifier. It has been demonstrated that if CO induces important resistances due mass transfer reaction at OCV, this phenomenon was less important under polarization. Indeed, the contribution of the electrodes, which was always superior to the electrolyte one at OCV, can decrease at 0.8V as low as 30% in the case of the wet (3% H<sub>2</sub>O) 20% H<sub>2</sub>-20%CO-10% CO<sub>2</sub>-50%N<sub>2</sub>, 17% H<sub>2</sub>-20%CO-3%CH<sub>4</sub>-60%N<sub>2</sub> or 17% H<sub>2</sub>-20%CO-3%CH<sub>4</sub>-10% CO<sub>2</sub>-50%N<sub>2</sub> mixtures. As a consequence, in order to further increase the cells performance, studies must be oriented towards electrolyte improvements.

## ACKNOWLEDGEMENT

The authors are thankful to ADEME (Agence de l'Environnement et de la Maîtrise de l'Energie) for financial support through the TITEC (Transfert pré-Industriel et Tests En Conditions réelles) project VALORPAC. M. Ricoul is thankful to ANRT (Association Nationale de la Recherche et de la Technologie) for awarding his CIFRE (Convention Industrielle de Formation par la Recherche) thesis in the S3D Compagny.

## REFERENCES

1. Levin D.B., Chahine R., 2010, Challenges for renewable hydrogen production from biomass, *Int. J. Hydrogen Energy*, vol. 35, pp. 4962-4969.
2. Razbani O., Assadi M., 2013, Performance of a bihydrogen solid oxide fuel cell, *Int. J. Hydrogen Energy*, vol. 38, pp. 13781-13791.
3. Leone P., Lanzini A., Santarelli M., Cali M., Sagnelli F., Boulanger A., Scaletta A., Zitella P., 2010, Methane-free biogas for direct feeding of solid oxide fuel cell, *J. Power Sources*, vol. 195, pp. 239-248.



4. Saule M., Jürgen K., Frank N., 2008, "BioCellus-Biomass Fuel Cell Utility System," Technische Universität München, Project summary.
5. Aravind P.V., de Jong W., 2012, Evaluation of high temperature gas cleaning options for biomass gasification product gas for solid Oxide Fuel Cell, *Progress in Energy and Combustion Science*, vol. 38, pp. 737-764.
6. Lamarche P., Tazerout M, Pavier F., Contribution to the experimental study and the modeling of the biomass staged gasification in fixed bed reactor, 2011, thesis, Nantes.
7. Bocci E., Sisinni M., Moneti M., Vecchione L., Di Carlo A., Villarini M., 2014, State of art of small scale biomass gasification power systems: a review of the different typologies, *Energy Procedia*, vol. 45, pp. 247-256.
8. Ricoul F., Le Gal La Salle A., Kerihuel A., Subrenat A., Joubert O., 2014, High temperature fuel cell fueled with syngas produced from biomass gasification for small scale CHP units, *Proceedings of the European Biomass Conference and Exhibition, Hamburg, 23-26 juin*
9. Lebreton M., Delanoue B., Baron E., Ricoul F., Kerihuel A., Subrenat A., Joubert O., Le Gal La Salle A., 2014, Effects of carbon monoxide, carbon dioxide, and methane on Nickel/Yttria-stabilized Zirconia-based Solid Oxide Fuel Cells performance for direct coupling with a gasifier, *Int. J. Hydrogen Energy*, submitted
10. Ihringer R., 2R-Cell : A universal cell for an easy and safe SOFC operation, *Electrochem Soc. Transactions*, vol. 35, pp. 393-402.
11. Huang Q.-A., Hui R., Wang B., Zhang J., 2007, A review of AC impedance modelling and validation in SOFC diagnosis, *Electrochim. Acta*, vol. 52, pp. 8144-8164.
12. Johnson D, ZView: A software program for IES analysis, Version 2.8, 2002, Scribner associates, INC, Southern Pines, NC.
13. Hornes A., Escudero M.J., Daza L., Martinez-Arias A., 2014, Electrochemical performance of a solid oxide fuel cell with an anode based on Cu-Ni/CeO<sub>2</sub> for methane direct oxidation, *J. Power Sources*, vol. 249, pp. 520-526.
14. Chockalingam R., Ganguli A.K., Basu S., 2014, Praseodymium and gadolinium doped ceria as a cathode material for low temperature solid oxide fuel cell, *J. Power Sources*, vol. 250, pp. 80-89.
15. Nielsen J., Hjelm J., 2014, Impedance of SOFC electrodes: A review and a comprehensive case study on the impedance of LSM:YSZ cathodes, *Electrochim. Acta*, vol. 115, pp. 31-45.
16. Marrero-Lopez D., Pena-Martinez J., Ruiz-Morales J.C., Gabas M., Nunez P., Aranda M.A.G., Ramos-Barrado J.R., 2010, Redox behaviour, chemical compatibility and electrochemical performance of Sr<sub>2</sub>MgMoO<sub>6-δ</sub> as SOFC anode, *Solid St. Ionics*, vol. 180, pp. 1672-1682.
17. Ju H., Eom J., Lee J.K., Choi H., Lim T-H., Song R-H, Lee J., 2014, Durable power performance of a direct ash-free coal fuel cell, *Electrochim. Acta*, vol 115, pp. 511-517.
18. J.R. MacDonald, *Impedance Spectroscopy Emphasizing Solid Materials and Systems*, 1987, Wiley, New York.
19. Bonanos N., *The application of impedance spectroscopy to solid oxide fuel cells and their components*, 2008, EIS-2008, 41st Heyrovsky Discussion, Caste Trest, Czech Republic.
20. Sun L-P., Zhao H., Li Q., Huo L-H., Viricelle J-P., Pijolat C., 2013, Study of oxygen reduction mechanism on Ag modified Sm<sub>1.8</sub>Ce<sub>0.2</sub>CuO<sub>4</sub> cathode for solid oxide fuel cell, *Int. J. Hydrogen Energy*, vol. 38, pp. 14060-14066
21. Marrero-Lopez D., Romero R., Martin F., Ramos-Barrado J.R., 2014, Effect of the deposition temperature on the electrochemical properties of La<sub>0.6</sub>Sr<sub>0.4</sub>Co<sub>0.8</sub>Fe<sub>0.2</sub>O<sub>3-δ</sub> cathode prepared by conventional spray-pyrolysis, *J. Power Sources*, vol 255, pp.308-317.
22. Leonide A., Sonn V., Weber A., Ivers-Tiffée E., 2008, Evaluation and Modeling of the cell resistance in anode-supported solid oxide fuel cell, *J. Electrochem. Soc.*, vol. 155, pp. B36-B41
23. Primdahl S., Mogensen M., 1999, Gas diffusion impedance in characterization of Solid Oxide Fuel cell anodes, *J. Electrochem. Soc.*, vol. 146, pp. 2827-2833.
24. M. Lo Faro, A. Vita, L. Pino, A.S. Arico, 2013, Performance evaluation of a solid oxide fuel cell coupled to an external biogas tri-reforming process, *Fuel Process. Techn.*, vol. 115, pp. 238-245.

# Coupling a biomass gasification process and a Solid Oxide Fuel Cell (SOFC)

F. Ricoul<sup>1</sup>, A. Le Gal La Salle<sup>2</sup>, O. Joubert<sup>2</sup>, A. Subrenat<sup>3</sup>, A. Kerihuel<sup>1</sup>

<sup>1</sup>S3D, 2 rue Alfred Kastler 44307 Nantes, France

<sup>2</sup>IMN, 2 rue de la Houssinière 44322 Nantes, France

<sup>3</sup>EMN, 4 rue Alfred Kastler 44307 Nantes, France

ricoul@sol3d.com

**Keywords: Solid Oxide Fuel Cell, Gasification process, Biomass**

Usually SOFC are fuelled with H<sub>2</sub> or CH<sub>4</sub>. To produce this kind of gas it's possible to use methanisation or gasification from fermentable or combustible biomass respectively. The interest of gasification includes the production of H<sub>2</sub> and CO from biomass or organic wastes in the temperature range (700-800°C) of the SOFC operating conditions. The gasification CHP units have a global electric yield ranging between 20 and 25%. With a SOFC in substitution of engine, the global electric yield can reach at least 30 to 40%. The key issue of this work is to find solutions for operating a SOFC fuelled with gas produced from biomass.

The first part of our work was to develop and build a gasification pilot unit according to the concept patented by S3D (Figure 1), delivering low tar containing gases. The gasification pilot unit is now mounted, and the analyses of the composition of the exhaust gases are in progress. At the same time Ni-YSZ-based SOFC are tested with synthetic gas with composition corresponding to the one of the exhaust gas of the gasifier. First results show that cells can successfully run when they are fuelled with N<sub>2</sub>, H<sub>2</sub>, CO, CO<sub>2</sub> and CH<sub>4</sub> mixtures. Experiments realized at 750°C show that the presence of H<sub>2</sub>S at concentrations as low as 2 ppm of H<sub>2</sub>S leads to a decrease of the performance of the cell (app. 20%) during the first 20 hours and followed by a stabilization. Fueling the cell again with a syngas without H<sub>2</sub>S leads to a partial recovering of its performance. On the contrary, the presence of HCl at concentrations from 5 to 200 ppm seems have no influence. Taking into account these results, it's possible to design a gas treatment unit related to SOFC specifications.

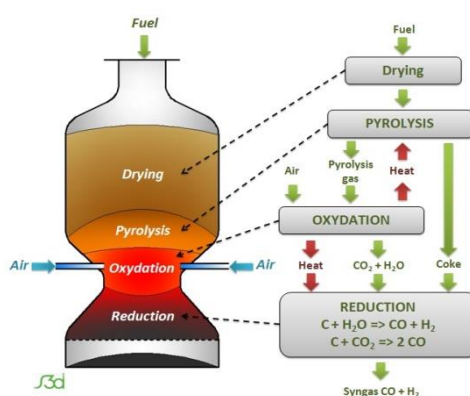


Figure 1. Principles of the downdraft gasifier

## REFERENCES

1. F. Ricoul, A. Le Gal La Salle, A. Kerihuel, A. Subrenat, O. Joubert, *Proceedings of the European Biomass Conference and Exhibition*, Hamburg, 23-26 juin 2014